

Artificial Tongue Based on Metal-Biomolecule Coordination Polymer Nanoparticles

Fang Pu, Xiang Ran, Jinsong Ren, Xiaogang Qu**

Experimental Section

Materials and methods.

Guanosine 5'-monophosphate (GMP), thioflavin T (ThT), thiazole orange (TO), pyronin Y (PY) were purchased from Sigma-Aldrich. N-Methylmesoporphyrin IX (NMM) was purchased from Porphyrin Products Inc (Logan, UT). Europium nitrate hexahydrate ($\text{Eu}(\text{NO}_3)_3 \cdot 6\text{H}_2\text{O}$) was purchased from Aladdin Reagent (Shanghai, China). All other reagents were all of analytical reagent grade and used as received.

Fluorescence spectra were measured on a JASCO FP-6500 spectrophotometer. Scanning electron microscopy (SEM) was conducted on an S-4800 field emission scanning microscope.

Preparation of GMP/dyes/Eu coordination polymer nanoparticles.

GMP (5 mM), dyes ($[\text{ThT}] = 30 \mu\text{M}$, $[\text{TO}] = 60 \mu\text{M}$, $[\text{PY}] = 5 \mu\text{M}$, $[\text{NMM}] = 5 \mu\text{M}$) and $\text{Eu}(\text{NO}_3)_3$ (2 mM) were mixed in aqueous solution under slight shake at room temperature. Solid products were formed immediately. The products were kept at room temperature for 30 min and collected by centrifugation.

Sensing studies.

For performing the array-based sensor, GMP/dye/Eu CPNs (10 μL) were introduced into 600 μL aqueous solution containing different metal ions at room temperature. Fluorescent spectra were measured individually by excitation at 440 nm, 490 nm, 546 nm, 399 nm, respectively. Then the fluorescent data were collected.

Identification of unknown samples.

The procedure of identification of unknown samples followed the procedure in previous reports.¹⁻³ Firstly, the known samples were prepared and tested. The PCA results of the known samples were utilized as training matrix for the identification of unknown samples. The unknown samples were prepared in the same manner as the

known samples and randomized by a different person. The sample identity was unknown during the analysis. The fluorescence responses of the sensor array to these unknown samples were then measured. The data were analyzed with PCA to identify the unknown samples by comparing the results with the training matrix.

Data Analysis.

The patterns were processed using principal component analysis (PCA) in MATLAB R2012a. Hierarchical cluster analysis (HCA) was carried out with the help of SYSTAT 13 (version 13.1).

Reference

1. S. Wang, L. Ding, J. Fan, Z. Wang and Y. Fang, *ACS Appl Mater Interfaces*, 2014, **6**, 16156.
2. Y. He, X. He, X. Liu, L. Gao and H. Cui, *Anal. Chem.*, 2014, **86**, 12166.
3. D. Wu and K. S. Schanze, *ACS Appl Mater Interfaces*, 2014, **6**, 7643.

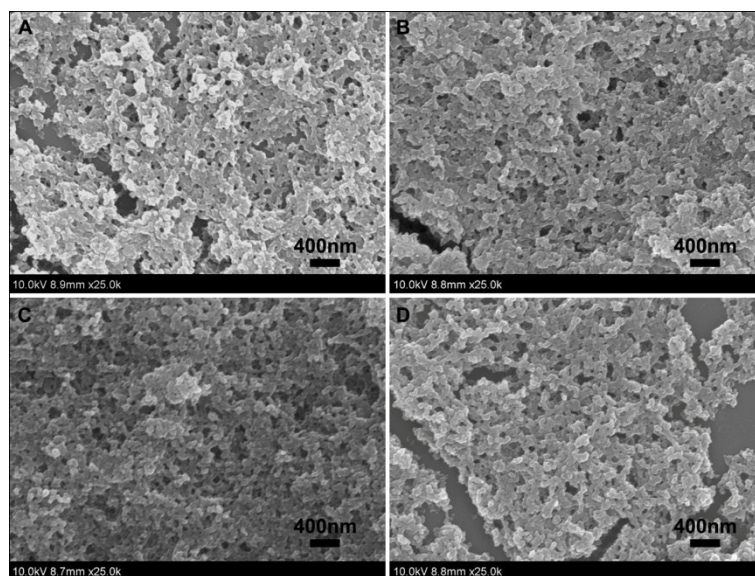


Figure S1 SEM images of (A) GMP/ThT/Eu, (B) GMP/TO/Eu, (C) GMP/PY/Eu, and (D) GMP/NMM/Eu.

Table S1 Excitation and emission wavelengths used for reporter molecules.

<i>Reporter</i>	<i>extinction coefficient</i> ($M^{-1} cm^{-1}$)	$\lambda_{excitation}$ (nm)	$\lambda_{emission}$ (nm)
ThT	36000 (412 nm)	440	488
TO	63000 (500 nm)	490	535
PY	103000 (545 nm)	546	565
NMM	145000 (379 nm)	399	612

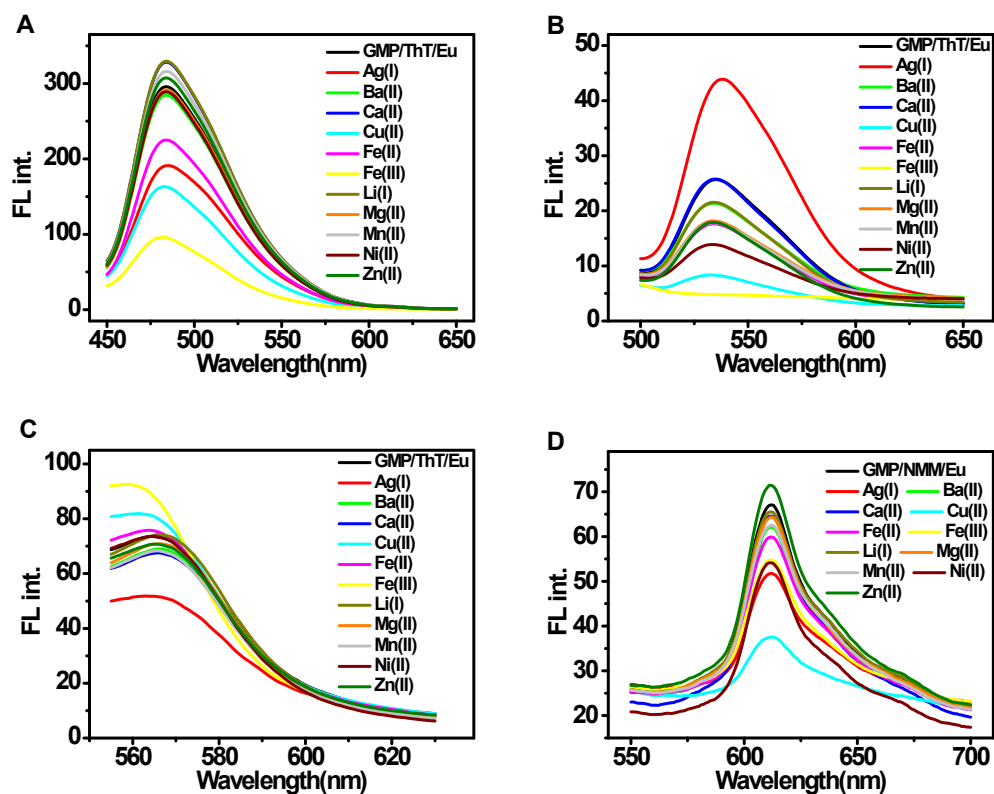


Figure S2 Fluorescence spectra (A) GMP/ThT/Eu, (B) GMP/TO/Eu, (C) GMP/PY/Eu, and (D) GMP/NMM/Eu upon addition of various metal ions. [metal ions] = 80 μM .

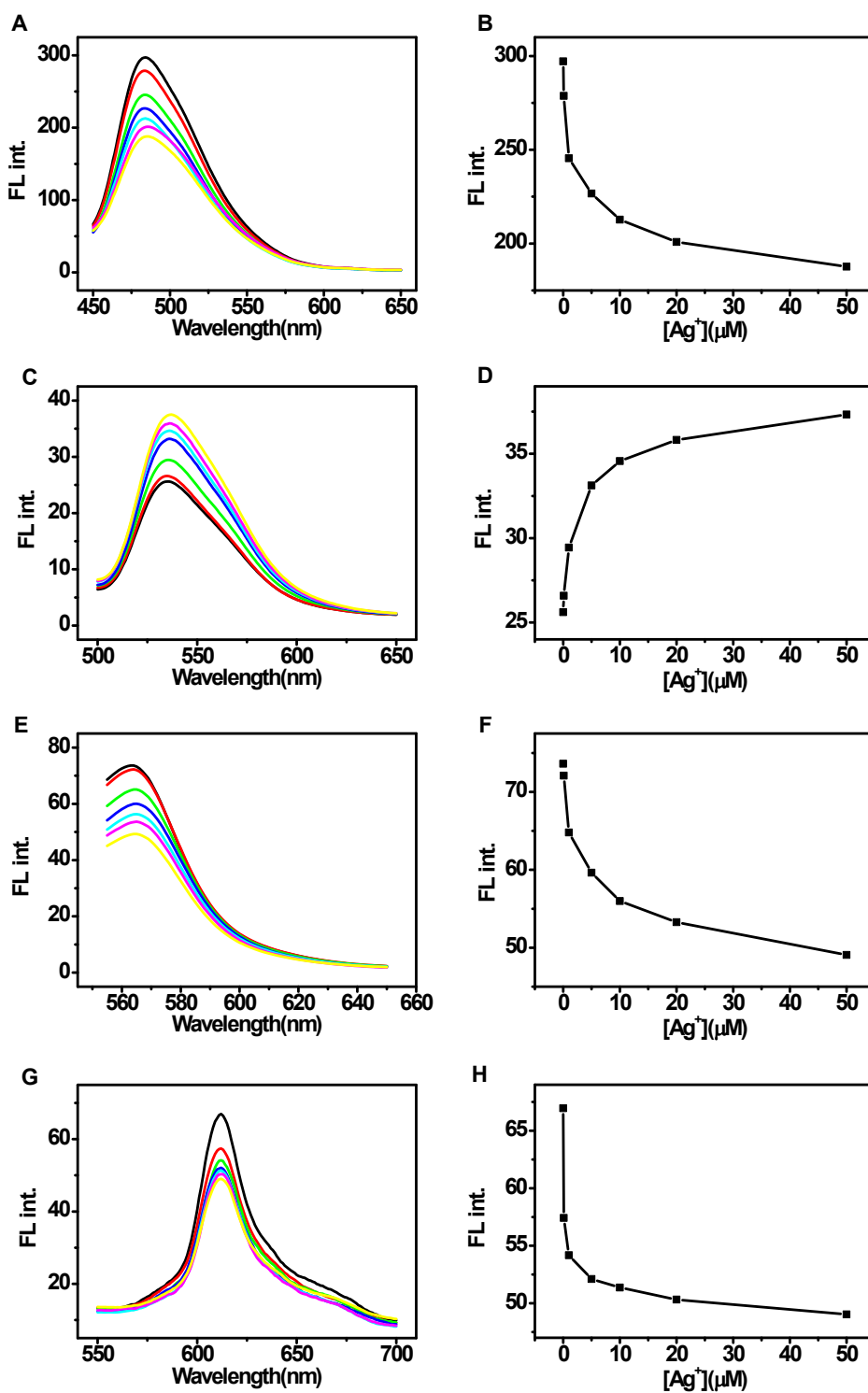


Figure S3 (Left) Fluorescence spectra of (A) GMP/ThT/Eu, (C) GMP/TO/Eu, (E) GMP/PY/Eu, and (G) GMP/NMM/Eu CPNs with increasing the concentration of Ag^+ . (Right) Plots of the fluorescence intensity at (B) 488, (D) 535, (F) 565, and (H) 612 nm as a function of the Ag^+ concentration.

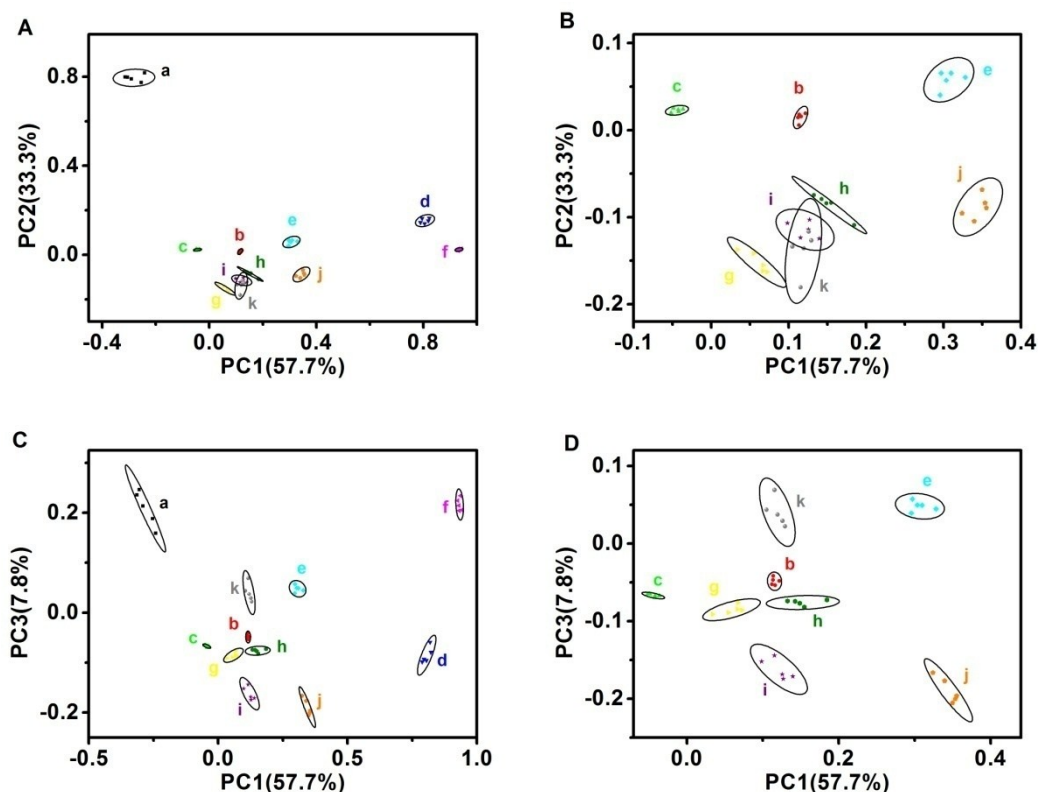


Figure S4 (A) Two-dimensional (2-D) plot showing projections of the clusters on the PC1-PC2 axes. (B) The enlarged 2-D plot of the metal ions including (b) Ba^{2+} , (c) Ca^{2+} , (e) Fe^{2+} , (g) Li^{+} , (h) Mg^{2+} , (i) Mn^{2+} , (j) Ni^{2+} and (k) Zn^{2+} . (C) 2-D plot showing projections of the clusters on the PC1-PC3 axes. (D) The enlarged 2-D plot of the metal ions including (b) Ba^{2+} , (c) Ca^{2+} , (e) Fe^{2+} , (g) Li^{+} , (h) Mg^{2+} , (i) Mn^{2+} , (j) Ni^{2+} and (k) Zn^{2+} ions. The ellipses indicate 95% confidence level.

The results suggested that the 2-D dimensional plot generated using PC1 and PC2 was sufficient to discriminate seven metal ions ((a) Ag^{+} , (b) Ba^{2+} , (c) Ca^{2+} , (d) Cu^{2+} , (e) Fe^{2+} , (f) Fe^{3+} , and (j) Ni^{2+}). The additional orthogonal dimension could further enhance separation ability, achieving complete discrimination of metal ions tested. Therefore, 3-D plot was generated using the first three most significant principal components to obtain better analyte discrimination.

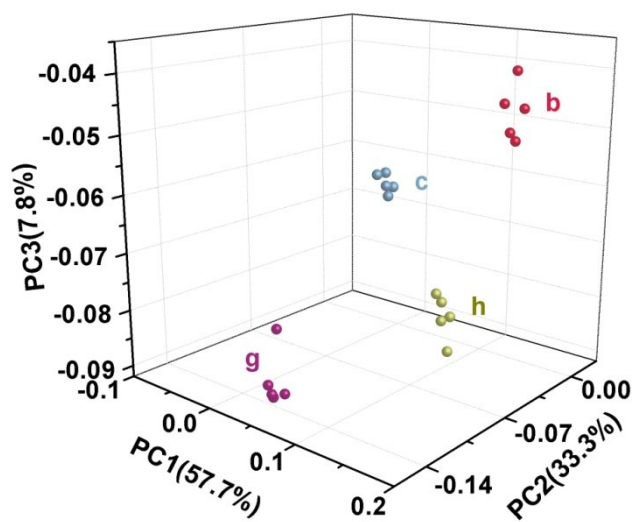


Figure S5 The enlarged 3-D plot of the metal ions including (b) Ba²⁺, (c) Ca²⁺, (g) Li⁺, and (h) Mg²⁺.

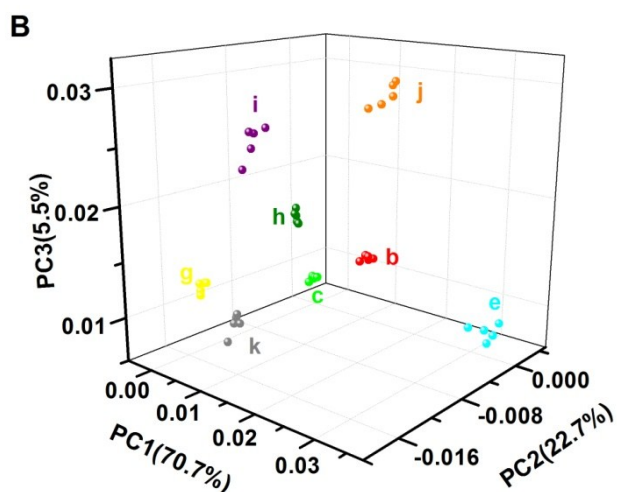
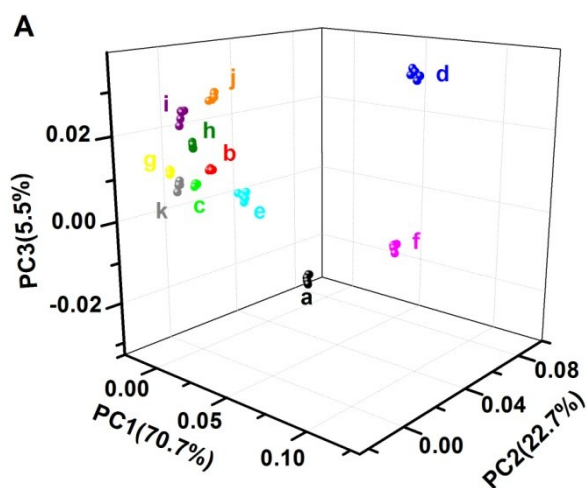


Figure S6 (A) 3-D PCA score plot derived from the fluorescence data. (a) Ag^+ , (b) Ba^{2+} , (c) Ca^{2+} , (d) Cu^{2+} , (e) Fe^{2+} , (f) Fe^{3+} , (g) Li^+ , (h) Mg^{2+} , (i) Mn^{2+} , (j) Ni^{2+} and (k) Zn^{2+} ions. [metal ions] = 0.4 μM . (B) The enlarged 3-D plot of the metals including (b) Ba^{2+} , (c) Ca^{2+} , (e) Fe^{2+} , (g) Li^+ , (h) Mg^{2+} , (i) Mn^{2+} , (j) Ni^{2+} and (k) Zn^{2+} ions.

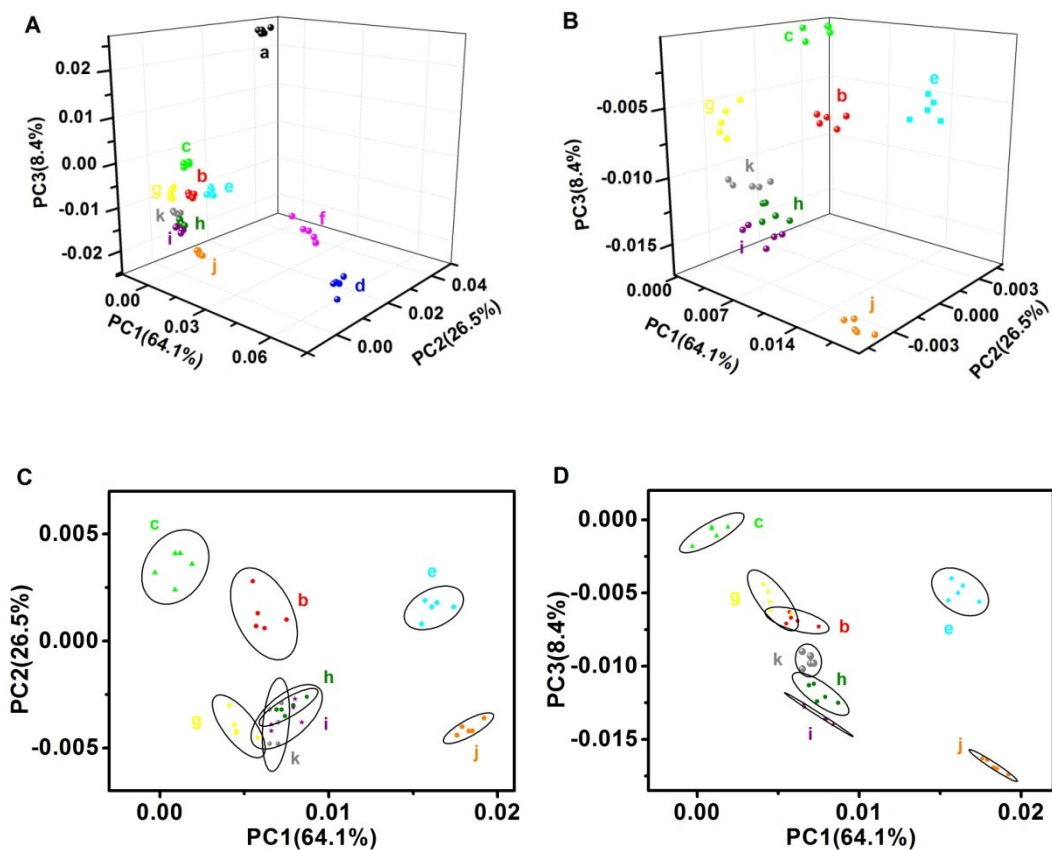


Figure S7 (A) 3-D PCA score plot derived from the fluorescence data. (a) Ag^+ , (b) Ba^{2+} , (c) Ca^{2+} , (d) Cu^{2+} , (e) Fe^{2+} , (f) Fe^{3+} , (g) Li^+ , (h) Mg^{2+} , (i) Mn^{2+} , (j) Ni^{2+} and (k) Zn^{2+} ions. $[\text{metal ions}] = 0.2 \mu\text{M}$. (B) The enlarged 3-D plot of the metals including (b) Ba^{2+} , (c) Ca^{2+} , (e) Fe^{2+} , (g) Li^+ , (h) Mg^{2+} , (i) Mn^{2+} , (j) Ni^{2+} and (k) Zn^{2+} ions. (C) The enlarged 2-D plot showing projections of the clusters including (b) Ba^{2+} , (c) Ca^{2+} , (e) Fe^{2+} , (g) Li^+ , (h) Mg^{2+} , (i) Mn^{2+} , (j) Ni^{2+} and (k) Zn^{2+} on the PC1-PC2 axes. (D) The enlarged 2-D plot showing projections of the clusters on the PC1-PC3 axes. The ellipses indicate 95% confidence level.

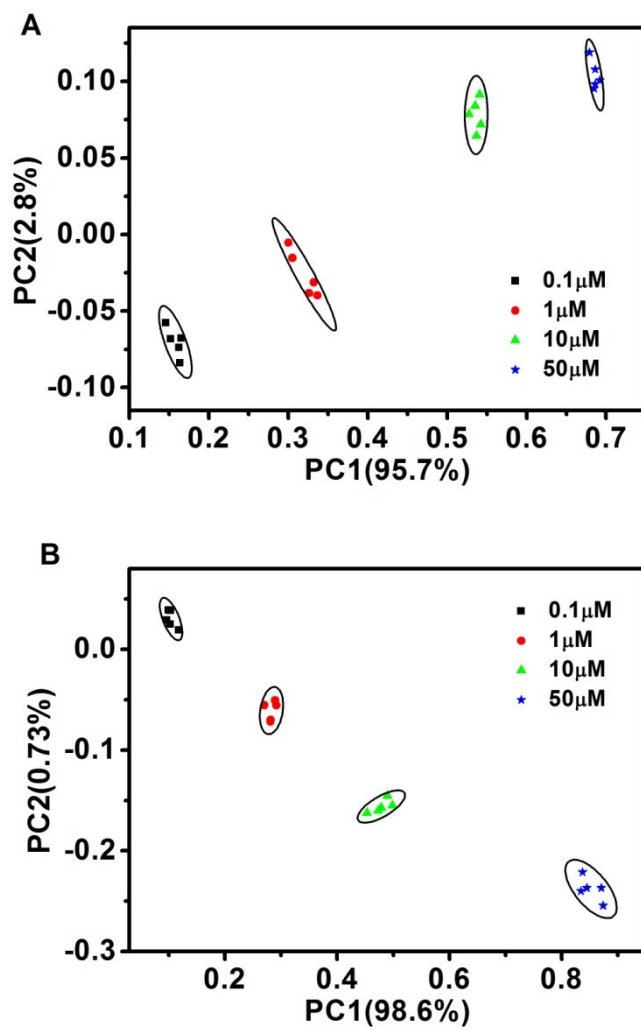


Figure S8 Score plots derived from (A) Ag^+ samples and (B) Cu^{2+} samples with different concentrations by PCA. The ellipses indicate 95% confidence level.

Table S2 The identifying results of 22 unknown samples.

The fluorescence data of four sensor receptors against 11 metal ions ((a) Ag⁺, (b) Ba²⁺, (c) Ca²⁺, (d) Cu²⁺, (e) Fe²⁺, (f) Fe³⁺, (g) Li⁺, (h) Mg²⁺, (i) Mn²⁺, (j) Ni²⁺ and (k) Zn²⁺ ions) with concentration of 80 μM were used as training matrix. The PCA plot was shown in Figure 3.

The 22 unknown samples with the same concentrations as the known samples ([metal ions] = 80 μM) were prepared by a different person and labeled randomly. The fluorescence responses from each unknown samples were collected and put into the training matrix generated in Figure 3 for identification. The Matlab program calculated the relativity of unknown response with known samples. Then the unknown samples were assigned as one of the metal ions or not recognized. The results were verified by the person who prepared the unknown samples.

Label	$(I_0-I)/I_0^a$				Identity	Prediction accuracy
	GMP/ThT/Eu	GMP/TO/Eu	GMP/PY/Eu	GMP/NMM/Eu		
1.	0.03783	0.28772	0.03553	-0.08831	Zn(II)	Y
2.	0.03791	0.17059	0.05802	0.07095	Ba(II)	Y
3.	-0.07417	0.18557	-0.00658	-0.0136	Li(I)	Y
4.	0.45972	0.66643	-0.08496	0.43231	Cu(II)	Y
5.	0.23594	0.28376	-0.01001	0.10365	Fe(II)	Y
6.	-0.04201	-0.00835	0.05903	0.03308	Ca(II)	Y
7.	0.68531	0.81519	-0.17466	0.19831	Fe(III)	Y
8.	0.02683	0.4435	-0.00344	0.19655	Ni(II)	Y
9.	-0.08868	0.1912	-0.02029	-0.0189	Li(I)	Y
10.	0.00246	0.29411	0.07082	0.03879	Mg(II)	Y
11.	-0.07694	0.32015	0.05765	0.05842	Mn(II)	Y
12.	0.39237	-0.68949	0.29385	0.25091	Ag(I)	Y
13.	0.04954	0.29595	0.05658	-0.07151	Zn(II)	Y
14.	0.39942	-0.69249	0.27591	0.24695	Ag(I)	Y
15.	0.67813	0.81669	-0.2162	0.21005	Fe(III)	Y
16.	-0.05605	0.00155	0.04123	0.11417	--	N
17.	-0.08098	0.29663	0.08273	0.04052	Mn(II)	Y
18.	0.47098	0.68046	-0.06989	0.45641	Cu(II)	Y
19.	0.21841	0.27225	-0.04782	0.09844	Fe(II)	Y

20.	0.03474	0.18082	0.0569	0.05328	Ba(II)	Y
21.	0.01519	0.29822	0.0423	0.05995	Mg(II)	Y
22.	0.05362	0.44207	0.00618	0.22977	Ni(II)	Y

^a I and I₀ are the fluorescent intensities at 488, 535, 565, and 612 nm corresponding to ThT, TO, PY, and NMM in the presence and absence of metal ions, respectively.